

# Radiance Preprocessing for Assimilation in the Hourly Updating Rapid Refresh Mesoscale Model: A Study Using AIRS Data

HAIDAO LIN

*NOAA/Earth System Research Laboratory, Boulder, and Cooperative Institute for Research in the Atmosphere,  
Colorado State University, Fort Collins, Colorado*

STEPHEN S. WEYGANDT

*NOAA/Earth System Research Laboratory, Boulder, Colorado*

AGNES H. N. LIM

*Cooperative Institute for Meteorological Satellite Studies, University of Wisconsin–Madison, Madison, Wisconsin*

MING HU

*NOAA/Earth System Research Laboratory, and Cooperative Institute for Research in Environmental Sciences,  
University of Colorado, Boulder, Colorado*

JOHN M. BROWN AND STANLEY G. BENJAMIN

*NOAA/Earth System Research Laboratory, Boulder, Colorado*

(Manuscript received 3 March 2017, in final form 16 July 2017)

## ABSTRACT

This study describes the initial application of radiance bias correction and channel selection in the hourly updated Rapid Refresh model. For this initial application, data from the Atmospheric Infrared Sounder (AIRS) are used; this dataset gives atmospheric temperature and water vapor information at higher vertical resolution and accuracy than previously launched low-spectral resolution satellite systems. In this preliminary study, data from AIRS are shown to add skill to short-range weather forecasts over a relatively data-rich area. Two 1-month retrospective runs were conducted to evaluate the impact of assimilating clear-sky AIRS radiance data on 1–12-h forecasts using a research version of the National Oceanic and Atmospheric Administration (NOAA) Rapid Refresh (RAP) regional mesoscale model already assimilating conventional and other radiance [AMSU-A, Microwave Humidity Sounder (MHS), HIRS-4] data. Prior to performing the assimilation, a channel selection and bias-correction spinup procedure was conducted that was appropriate for the RAP configuration. RAP forecasts initialized from analyses with and without AIRS data were verified against radiosonde, surface atmosphere, precipitation, and satellite radiance observations. Results show that the impact from AIRS radiance data on short-range forecast skill in the RAP system is small but positive and statistically significant at the 95% confidence level. The RAP-specific channel selection and bias correction procedures described in this study were the basis for similar applications to other radiance datasets now assimilated in version 3 of RAP implemented at NOAA's National Centers for Environmental Prediction (NCEP) in August 2016.

---

 Denotes content that is immediately available upon publication as open access.

---

*Corresponding author:* Haidao Lin, [haidao.lin@noaa.gov](mailto:haidao.lin@noaa.gov)

## 1. Introduction

The Atmospheric Infrared Sounder (AIRS), launched in May 2002 on the National Aeronautics and Space Administration (NASA) Earth Observing System (EOS)

DOI: 10.1175/WAF-D-17-0028.1

© 2017 American Meteorological Society. For information regarding reuse of this content and general copyright information, consult the [AMS Copyright Policy \(www.ametsoc.org/PUBSReuseLicenses\)](http://www.ametsoc.org/PUBSReuseLicenses).

polar-orbiting *Aqua* platform, is a 3.7–15.4- $\mu\text{m}$  infrared spectrometer with 2378 spectral channels and 13.5-km horizontal resolution at nadir (Aumann et al. 2003). By measuring radiation in more than 2000 different channels, AIRS provides atmospheric temperature and water vapor information at higher vertical resolution than previous low-spectral-resolution infrared satellite sounders.

The purpose of this study is to document the impact of assimilating AIRS clear-sky radiance data into the hourly updated National Oceanic and Atmospheric Administration (NOAA) operational Rapid Refresh (RAP; Benjamin et al. 2016) model system to assess its impact on very short-range (3–12 h) forecasts and to set the stage for other radiance data assimilation within RAP. This study was conducted in preparation for operational assimilation of AIRS radiance data and other hyperspectral sounder data in the hourly updated operational RAP model system implemented at the National Centers for Environmental Prediction (NCEP). Although the positive impacts of AIRS have been well documented in global prediction systems and some regional prediction systems, they have not been documented for more frequently updated systems like RAP for very short-term forecasts (0–12 h). RAP-appropriate channel selection and bias correction techniques applied in this study are the basis of similar techniques applied to other radiance datasets in version 3 of RAP (RAPv3) that was implemented in August 2016, in which hourly real-time satellite radiance data have been shown to have small positive impact with statistical significance (Lin et al. 2017).

Assimilation of AIRS data into global numerical weather prediction (NWP) systems has been shown in many studies to improve model initial conditions, leading to more accurate forecasts over the last decade. ECMWF first operationally assimilated AIRS radiances in September 2003 (McNally et al. 2006). The initial improvements in forecast skill for global 500-hPa geopotential height were small but consistent, with a larger-magnitude improvement in the Southern Hemisphere. The Met Office (UKMO; Cameron et al. 2005) began assimilating AIRS radiances on 26 May 2004. Verification against observations and analysis fields showed 0.4%–0.5% improvements in the UKMO NWP index (<http://www.metoffice.gov.uk/research/weather/numerical-modelling/verification/uk-nwp-index-doc>). Using the NCEP verification system, Le Marshall et al. (2006) reported that AIRS data had a consistent and beneficial effect on 500-hPa geopotential height forecast skill over the Southern Hemisphere, with a decrease in the 500-hPa height correlation between the forecast and the verifying analysis to below 0.60 being delayed by

about 6 h when AIRS data were assimilated (their Fig. 2). A slightly smaller-magnitude improvement in forecast skill was seen in the Northern Hemisphere. This was attributed to the dense conventional observation network over North America, Europe, and Asia, so that there is less additional information added by AIRS data than where conventional observations are more sparse. Preoperational trials with AIRS assimilation at the Navy Research Laboratory (NRL) (Ruston et al. 2006) showed that an AIRS assimilation run produced slightly positive impacts in the Southern Hemisphere 500-hPa height anomaly correlation when compared to the control experiment. This positive impact led to the implementation of AIRS assimilation into their global models. Ota et al. (2013) showed a fairly strong impact from AIRS radiances in an ensemble forecast sensitivity to observations (EFSO) study using a more recent GFS ensemble data assimilation. Joo et al. (2013) showed that the impacts per sounding from *MetOp-A*/Infrared Atmospheric Sounding Interferometer (IASI) and AIRS are larger than those of the microwave sounders using the adjoint-based sensitivity method within the Met Office global NWP system. This study is not meant to provide a comparative impact from different satellite instruments in RAP but to demonstrate a successful initial application of channel selection and bias correction appropriate for the RAP radiance assimilation.

A small positive impact on short-term (0–72 h) forecasts has also been seen from AIRS radiance data when assimilated in regional models (McCarty et al. 2009; Singh et al. 2012; Lim et al. 2014; Wang et al. 2015). Using the framework mimicking that of the operational North American Mesoscale Forecast System (NAM), McCarty et al. (2009) showed at 48 h a forecast improvement in geopotential height at 500 hPa, defined as the time difference in hours at which the forecasts fall below two points of equal anomaly correction, is 2.3 h. They also showed improvement of 8% and 7% in equitable threat and bias scores of precipitation forecasts of 25 mm (6 h)<sup>-1</sup>. Using a similar framework, Lim et al. (2014) showed improvement in the temperature and radiance brightness temperature bias when compared with rawinsondes and satellite observations, respectively, using the tuned community Gridpoint Statistical Interpolation (GSI) assimilation system and the Weather Research and Forecasting (WRF) Model.

Limited satellite data coverage and effective design for regional radiance bias corrections (BCs) are key challenges for assimilating AIRS (and other satellite) data into limited-area and frequently updated models (with their associated short data-cutoff time). The non-uniform data coverage due to the limited extent of the domain and the limited data swaths from the polar

satellite orbits result in a highly variable number of available observations per cycle. The short observation cutoff time associated with the hourly cycle reduces the number of observations. The lower model top in RAP (10 hPa) compared to global models such as the NCEP Global Forecast System (GFS; 0.3-hPa model top) limits the channels for which radiance measurements can be assimilated into the model. These limitations can reduce the effectiveness of the radiance bias correction method employed.

We applied channel selection and a bias correction with spinup over a longer period prior to the assimilation to address these difficulties. We also considered a best-case (maximum) observation coverage scenario that neglects the data latency and cutoff issues described earlier. As such, the results presented in this paper represent an upper limit (in terms of maximum data coverage, subject to other limitations in this study) on the forecast improvement to be expected. The overall satellite clear-sky radiance data impact within RAP using the operational real-time datasets is documented in Lin et al. (2017).

In this paper, a brief description of the RAP model system is presented in section 2a, and retrospective experiment configurations are given in section 2b. AIRS channel selection and bias correction procedures for RAP are described in section 3. In section 4, results from the retrospective AIRS radiance assimilation experiments are presented. A summary and our conclusions are presented in section 5.

## 2. Experiment design

### a. Rapid Refresh model/assimilation system

The RAP mesoscale assimilation and forecast system was developed by the Global Systems Division (GSD) of NOAA's Earth System Research Laboratory (ESRL) in collaboration with the National Weather Service (NWS) and has run operationally at NCEP/NWS since 2012. The RAP configuration as it is used operationally at NCEP is described in Benjamin et al. (2016, hereafter B16). In this study, a slightly older version of RAP is used. We include here details about RAP where these are germane to this study and when they differ from the description in B16.

The RAP domain (for RAP versions 1 and 2) used in this study covers all of North America, including Alaska, Canada, Puerto Rico, and the adjacent ocean areas (see Fig. 1, domain valid for RAP versions 1 and 2). It has a 13-km horizontal resolution, with  $795 \times 567$  grid points and 50 vertical computational layers, as well as a 10-hPa model top. RAP utilizes the GSI (Wu et al. 2002; Kleist

et al. 2009) procedure for the analysis component and the Advanced Research version of WRF (WRF-ARW; Skamarock et al. 2008) for the forecast component. In addition to conventional data, satellite radiance data [Advanced Microwave Sounding Unit (AMSU-A), High-Resolution Infrared Radiation Sounder (HIRS-4), and Microwave Humidity Sounder (MHS)] are also assimilated in RAP through the Community Radiative Transfer Model (CRTM; Han et al. 2006; Weng 2007; Chen et al. 2008) incorporated within GSI. Only the variational option within GSI is used in this study; the hybrid three-dimensional variational data assimilation (3DVAR)–EnKF option is not activated. NCEP GFS model forecast atmospheric fields are introduced twice daily into RAP through two partial cycles (0300–0800 and 1500–2000 UTC). As described in B16, these partial cycles are hourly cycles that run alongside the ongoing main cycle and replace the ongoing cycle's 1-h forecast as the atmospheric background fields for the 0900 and 2100 UTC analyses. The surface fields (e.g., snow cover, soil temperature, and moisture) are continuously cycled independent of the GFS.

### b. Retrospective configuration

To evaluate the impact of AIRS radiance data, two retrospective runs, a control (CNTL) without AIRS and an experiment (EXP) with AIRS, were conducted over a 1-month (1–31 May 2010) period. These CNTL and EXP runs were started at 0300 UTC on 1 May 2010 when the GFS initial conditions for the atmosphere were introduced into RAP through a partial cycle. As with the full cycles, the EXP partial cycles used all data, including the AIRS radiance data, and the CNTL used all data but excluding the AIRS radiance data. To reduce computational resources, a 3-h cycling configuration was adopted instead of the hourly cycling used operationally. A 12-h forecast is produced for each 3-h cycle, yielding a total of 245 forecasts from which the average impact scores were computed. The complete list of observations assimilated in the CNTL is given in Table 1. This includes all available conventional data, as well as satellite radiance data from the AMSU-A, MHS, and HIRS-4. This matches the observation assimilation in RAP version 2 (B16), implemented at NCEP in February 2014. Inclusion of the other satellite radiance data and all the conventional observations is important for assessing the impact of AIRS within the full mix of observations.

The EXP run included the assimilation of all of the observations used in the CNTL run plus the AIRS radiance data. In this study, the conventional data used in these experiments were derived from the RAP real-time Binary Universal Form for Representation of

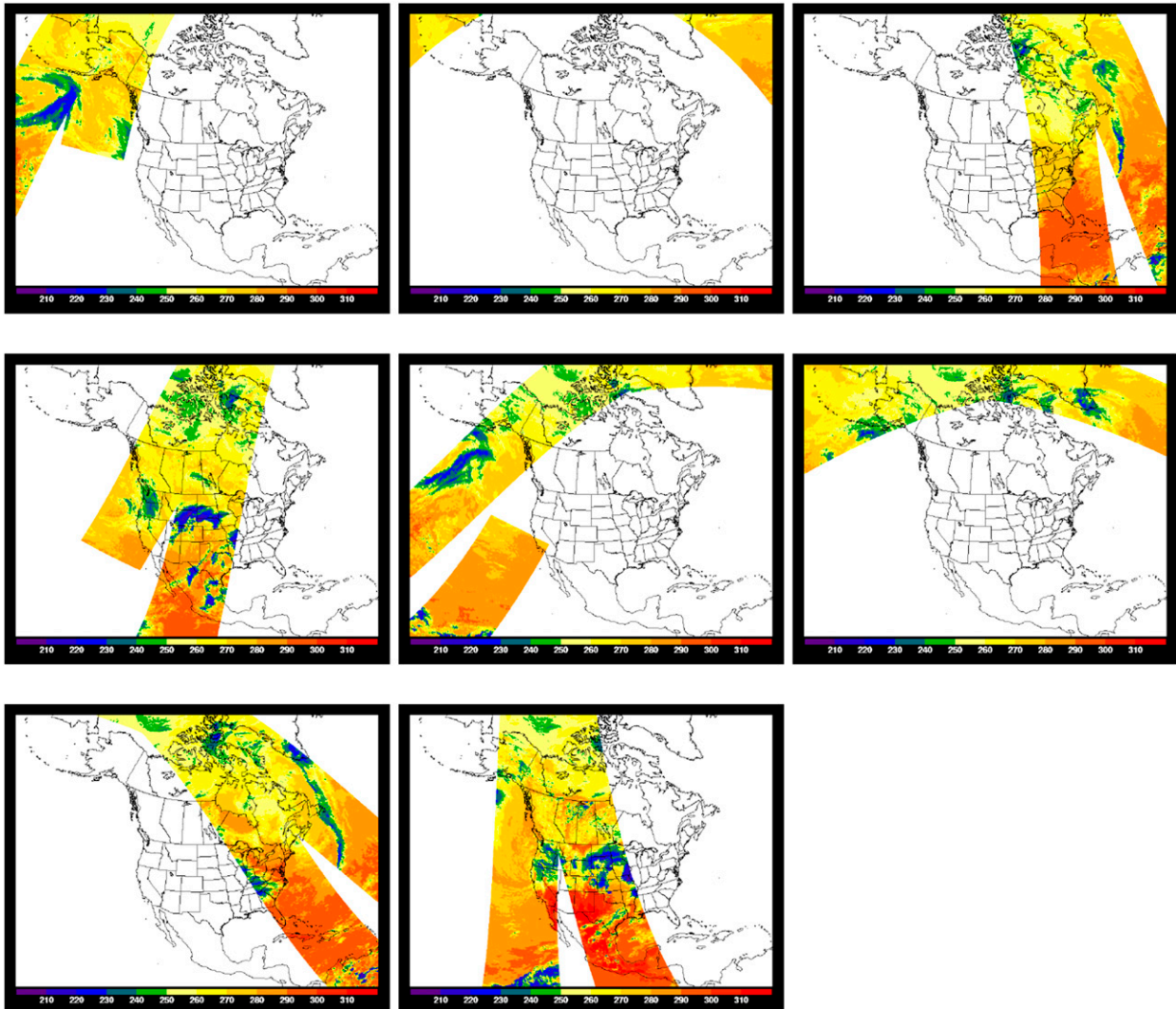


FIG. 1. AIRS observed BT (K) from channel 791 plotted onto the RAP domain for each cycle (3-h cycle) on 10 May 2010, starting with (top left) 0000 UTC, (top center) 0300 UTC, and then through 0600, 0900, 1200, 1500, 1800, and 2100 UTC.

Meteorological Data (BUFR) files from NCEP. For this study, we used the satellite radiance BUFR files from the NCEP Global Data Assimilation System (GDAS), which had a 6-h cutoff time and included radiances for the instruments (AMSU-A, MHS, HIRS-4, and AIRS) used in this study. In these experiments, full-coverage (i.e., assuming no data latency) AIRS data (only in the AIRS experiment, not in the control run), as well as other clear-sky radiance data, were assimilated using a 3-h time window. This full data coverage should provide a best-case scenario for the potential AIRS impact. Figure 1 shows the AIRS-observed brightness temperature from channel 791 (wavelength of  $10.88 \mu\text{m}$ ) for each cycle on 10 May 2010. There is good coverage (without real-time data latency and cutoff issues) over

the RAP domain for the AIRS data at 0600, 0900, 1200, 1800, and 2100 UTC.

A thinning procedure to  $60 \text{ km} \times 60 \text{ km}$  boxes was used for all radiance data in this study, as radiance observation errors are assumed to be spatially uncorrelated. For AIRS data, various interchannel checks (see section 3a) are used to do the thinning more intelligently by focusing on the clearest fields of view. The assumed observation errors used for all radiance channels assimilated in this study matched those from the GDAS.

### c. Verification

Forecasts initialized using analyses with and without assimilation of AIRS clear-sky radiances are verified

TABLE 1. Types of data used in the CNTL experiment.

Observation		Platform
Upper air	Conventional	Sonde Profiler Aircraft
Land surface		METAR Mesonet
Marine surface		Ship Buoy
Radar		VAD wind
Satellite winds [atmospheric motion vector (AMV)]	Satellite	GOES
Precipitable water		GPS
Microwave radiances		AMSU-A MHS
Infrared radiances		HIRS-4

against various observations to assess the impact from AIRS data on short-range forecasts. Observations used for verification included rawinsondes, METAR surface observations, NCEP Stage IV multisensor precipitation data (Lin and Mitchell 2005), and satellite observations.

The rawinsonde verification procedure used in this study follows Benjamin et al. (2004a), Benjamin et al. (2010), and Moninger et al. (2010). Approximately 8680 rawinsonde profiles (140 stations for each of 62 observation times) over the RAP domain were used in the verification. Root-mean-square (RMS) errors and mean errors (biases) were computed from forecast minus observed ( $F - O$ ) differences for temperature  $T$  and relative humidity (RH) at 3-, 6-, 9-, and 12-h forecast lengths. We further illustrate the impact of AIRS data on short-range forecasts by also expressing this difference as a percentage of the control forecast error. Percentage impacts are computed using a method described by Benjamin et al. (2004b) that does not consider observation errors or representativeness issues. This method yields a more conservative percentage change estimate than would be obtained by including these factors. The percentage impact is calculated as

$$x = \frac{(\text{CNTL} - \text{EXP})}{\text{CNTL}} \times 100, \quad (1)$$

where EXP is the average forecast RMS score (for different atmospheric layers; see below) for the experiment with AIRS and CNTL is the average forecast RMS score for the experiment without AIRS data. Using this definition, forecast improvements (error reduction) for a given experiment are indicated by a positive percentage impact. Verification is also conducted for different

atmospheric layers. The 1000–100-hPa vertical domain used for verification is partitioned into three layers: 1000–800 hPa (dominated by the boundary layer and surface effects), 800–400 hPa (the middle troposphere), and 400–100 hPa (from the upper troposphere to lower stratosphere, including the tropopause and upper-level jet maxima). The uncertainty of the RMS differences is estimated from the mean standard error, and differences of two standard errors are significant at the 95% confidence level. It is also noted that the double-difference series have been corrected with the lag-1 autocorrelation. More details about the uncertainty, lag-1 autocorrelation, and statistical significance can be found in Benjamin et al. (2010).

METAR surface observations [~2000 hourly reports in the continental United States (CONUS) domain] and NCEP Stage IV multisensor precipitation data (Lin and Mitchell 2005) are also used for verification of the RAP forecasts. For surface verification, the error percent reduction using Eq. (1) and bias comparison for 3-, 6-, 9-, and 12-h forecasts are calculated. For precipitation verification, 24-h accumulated precipitation forecast performance is evaluated using the critical success index (CSI; Schaefer 1990) scores and precipitation bias.

In addition, using CRTM, simulated satellite brightness temperature observations for AMSU-A on NOAA-18 and MHS on NOAA-19 are computed from forecast fields and then compared to real observations. To avoid errors between measurements and simulations brought about from large differences between time of observation and model valid time, a maximum time discrepancy of 30 min is allowed between the forecast fields and the observations. Biases computed for different forecast hours (3–12 h) are used to assess the forecast improvement due to the assimilation of AIRS radiances.

### 3. AIRS channel selection for RAP and bias correction

#### a. AIRS channel selection for RAP

NOAA's National Environment Satellite, Data, and Information Service (NESDIS) distributes a reduced set (281-channel subset) of AIRS channels, selected by the AIRS science team (Susskind et al. 2003), to NWP centers for use in operational weather prediction in near-real time (NRT) (Goldberg et al. 2003). Because the RAP system has a relatively low model top of 10 hPa, satellite channels with a peak weighting function (PWF) that are near or above this level are not assimilated. A subset of 68 AIRS channels (from the NCEP GDAS 120-channel set) has been selected for use in the RAP assimilation based on an adjoint sensitivity

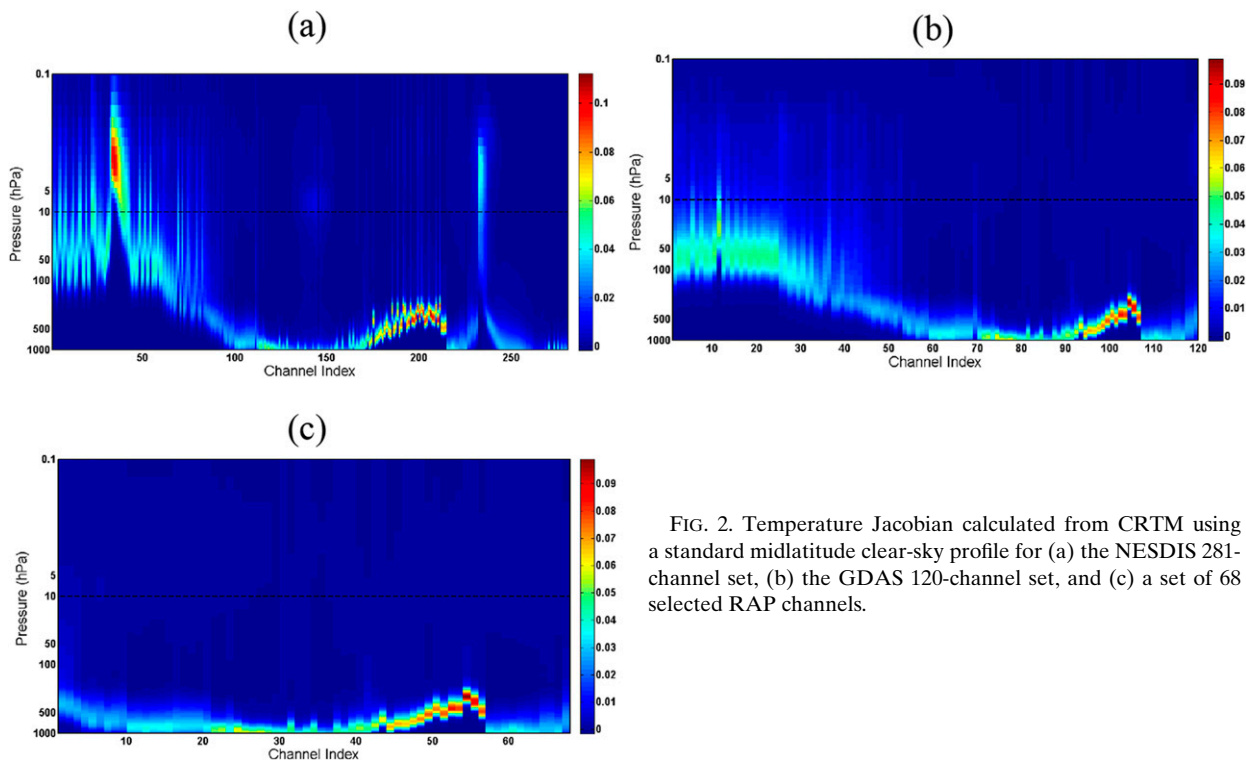


FIG. 2. Temperature Jacobian calculated from CRTM using a standard midlatitude clear-sky profile for (a) the NESDIS 281-channel set, (b) the GDAS 120-channel set, and (c) a set of 68 selected RAP channels.

analysis that was completed as part of this study and followed the method of [McCarty et al. \(2009\)](#). Based on this analysis, channels determined to have a significant contribution from levels above the RAP model top were

removed. Specifically, first of all, the brightness temperature sensitivity for each channel was calculated through multiplying the temperature Jacobian (calculated from CRTM through a midlatitude clear-sky profile) and a

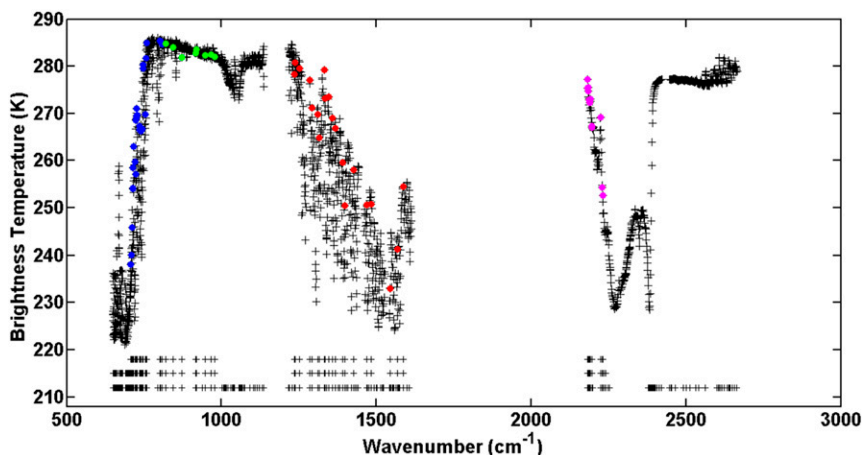


FIG. 3. An illustration of the AIRS spectrum (plus symbols; BT simulated from CRTM using a standard midlatitude clear-sky profile) and 68 selected channels (colors) for RAP, with blue indicating the selected CO<sub>2</sub> longwave channels (15  $\mu\text{m}$ ), green indicating the surface channels, red indicating the water vapor channels, and magenta indicating the CO<sub>2</sub> shortwave channels (4  $\mu\text{m}$ ). The bottom row of black plus (+) symbols indicates the 281 operational selected channels delivered to NCEP. The middle row of black plus symbols indicate 120 selected channels for the NCEP operational GDAS model. The top row of black plus symbols indicate the selected 68 channels for RAP.

TABLE 2. List of AMSU-A, MHS, and HIRS-4 channels used in the retrospective runs.

Satellite	Sensor	Channels assimilated
NOAA-15	AMSU-A	1–10 and 15
NOAA-18	AMSU-A	1–8, 10, and 15
	MHS	1–5
NOAA-19	AMSU-A	1–7, 9–10, and 15
MetOp-A	AMSU-A	1–6, 8–10, and 15
	MHS	1–5
	HIRS-4	4–8 and 10–15

finite perturbation (1% for temperature). Then, the total contribution from above the top of the model (10 hPa) to the top of the atmosphere (0.01 hPa) was calculated as the sum of the brightness temperature sensitivity from the levels above the model top to the top

of the atmosphere. If the value of the total contribution from the model top to the top of the atmosphere exceeded 0.06 K, then this channel was discarded. More details of this channel selection method may be found in [McCarty et al. \(2009\)](#). Figure 2 shows the temperature Jacobian of the 281 NESDIS NRT channel set, 120 GDAS channel set, and the newly selected RAP 68-channel set. It is apparent from [Figs. 2b and 2c](#) that the channels with peak values of the temperature Jacobian between around 10 and 100 hPa were removed. The remaining 68 channels were considered appropriate for assimilation into RAP with its 10-hPa model top. Figure 3 shows an example of the AIRS spectrum with the selected AIRS channels for RAP use. Blue dots represent the 15- $\mu\text{m}$  longwave carbon dioxide channels, green dots represent surface channels, red dots represent water vapor channels, and magenta dots represent

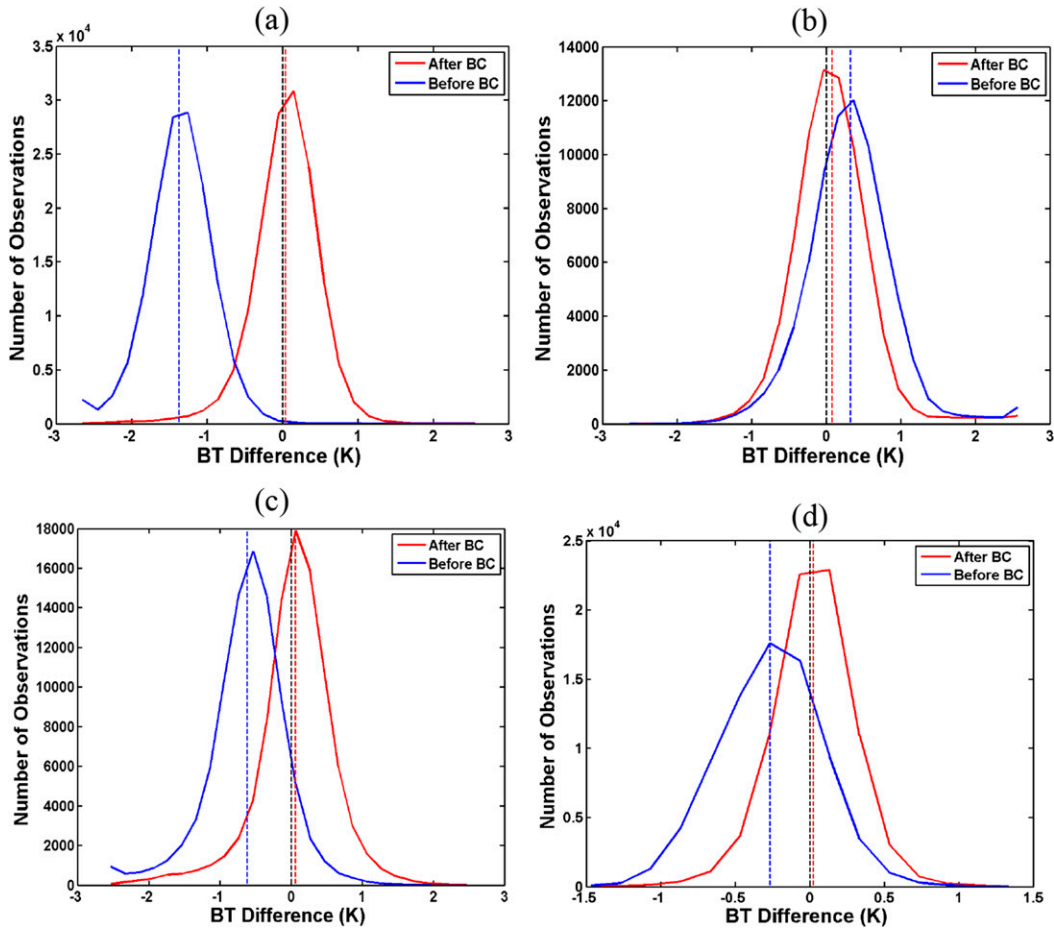


FIG. 4. Histogram of O-B values before (blue) and after BC for (a) AIRS channel 252 (longwave carbon dioxide channel with PWF height around 628 hPa), (b) AIRS channel 787 (surface channel), (c) AIRS channel 1382 (water vapor channel with PWF height around 840 hPa), and (d) AIRS channel 1881 (shortwave carbon dioxide channel with PWF height at around 695 hPa) from the AIRS experiment. Statistics are obtained from the 1-month experiments. The dashed blue line indicates the mean value for the blue line and the dashed red line indicates the mean value for the red line. The thick-dashed black line is the zero line.

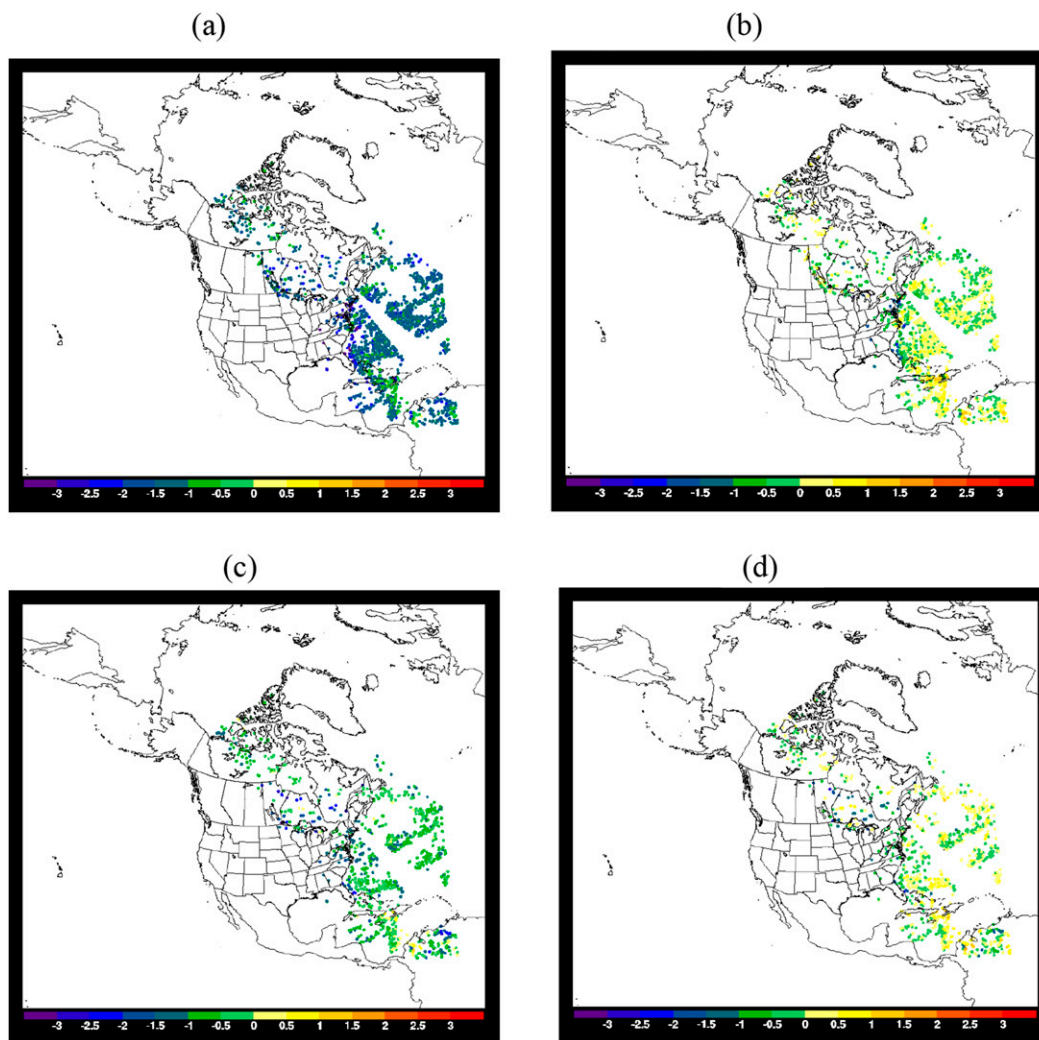


FIG. 5. BT difference (O-B) between the observed and background simulated at 1800 UTC 15 May 2010 for (a) before and (b) after BC for AIRS channel 252 (longwave carbon dioxide channel with PWF height around 628 hPa) and for (c) before and (d) after BC for AIRS channel 1382 (water vapor channel with PWF height around 840 hPa).

the  $4.3\text{-}\mu\text{m}$  shortwave carbon dioxide channels. The wavenumber of the 281 NRT channels, the 120 GDAS channels, and the 68 channels selected for this study are indicated by the black plus symbols in the lower portion of Fig. 3. Impact studies (not shown) using 9-day retrospective experiments showed slight improvements in upper-level (above 200 hPa) temperature forecasts and middle-level (800–600 hPa) moisture forecasts using this newly selected 68-channel set compared to assimilation without this channel selection (i.e., the GDAS 120-channel set). This led to the use of this newly selected channel set in this study. Channel selection for other radiance data (AMSU-A, MHS, and HIRS-4) has also been performed for RAP, leading to the removal of the high-level and ozone channels. The channels

(excluding AIRS data) assimilated in this study are listed in Table 2. More details about the channel selection procedures for AMSU-A, MHS, and HIRS-4 in RAP can be found in Lin et al. (2017).

It is noted that the assimilated AIRS radiance data passed the quality control and cloud detection procedures in GSI to remove the cloud-contaminated data. Over land and water, GSI uses three different threshold tests from the differences of shortwave and longwave thermal channels to identify clouds (Goldberg et al. 2003). For water surfaces, GSI uses the difference between model SST and AIRS window channel estimated SST for the initial clear test (Goldberg et al. 2003; Le Marshall et al. 2006). Then, a low-cloud/cirrus check is performed using the difference between  $3.4\text{-}\mu\text{m}$

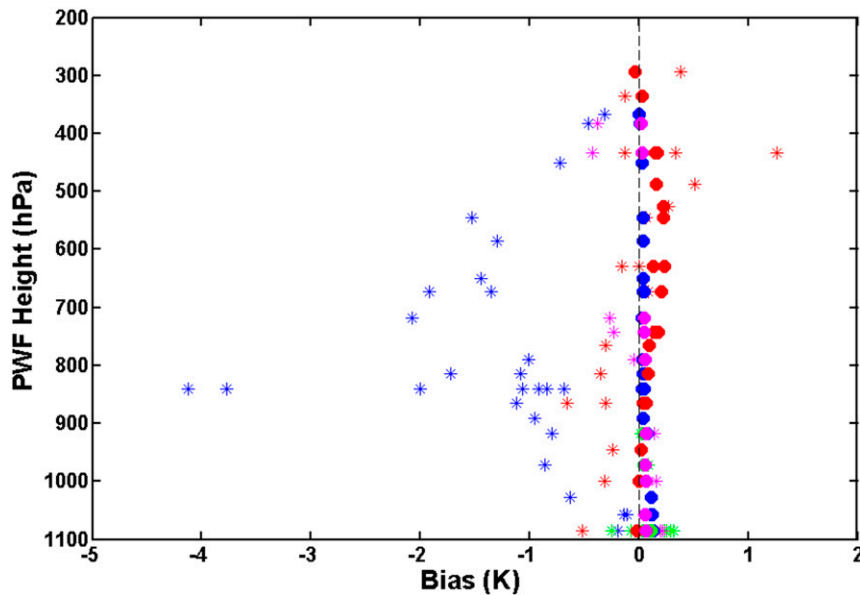


FIG. 6. Mean O-B (BT) values before [asterisks (\*)] and after (filled circles) BC for the 68 channels used over the 1-month AIRS experiment period. The 68 AIRS channels are arranged vertically by PWF height with blue indicating longwave carbon dioxide channels, green indicating surface channels, red indicating water vapor channels, and magenta indicating short-wave carbon dioxide channels.

channels (Le Marshall et al. 2006). In addition, a channel-dependent cloud check is performed based on the contribution from transmittance below the cloud-top level. If the transmittance of a channel from the cloud layer is more than 2%, then this channel is rejected. Data surviving these stringent procedures were assumed to be unaffected by clouds and therefore are eligible for assimilation.

#### b. Bias correction

Calibration-based biases in satellite radiances, if not corrected, are sources of error in an NWP assimilation system. These biases can vary with time, geographical location, air mass, and scan angle (Auligné et al. 2007). Within GSI, this is accomplished with a variant of the variational bias correction scheme described by Derber and Wu (1998), Dee (2005), and Zhu et al. (2014). For the GSI version used in this study, the bias correction is a two-step procedure. A dynamically updated air mass component modeled through predictors is included in the variational scheme. The coefficients of the air mass are updated during each assimilation. The scan-angle component is updated outside of the GSI and performed after running GSI.

Optimizing radiance bias correction in rapidly updated regional models is challenging as a result of the limited extent of the domain and nonuniform data coverage in space and time, as well as the relatively low

model top in RAP. The number of observations is highly variable from cycle to cycle and because of the timing of polar orbiter satellite passes relative to the limited domain, this sparse and highly variable data coverage adversely affects the variational BC procedures. BC procedures require a large observation sample size, as coefficients of predictors used to describe the biases are regressed against observations (Auligné et al. 2007). In addition, the relatively low model top can result in an insufficient description of the atmospheric structure, especially in upper levels, resulting in unrealistic observation innovations. One method of ameliorating this is to exclude observations with large innovations as part of the quality control (QC), but this further reduces the number of assimilated observations and can cause a negative feedback to the next cycle, leading to a degradation of the cycled analysis (Auligné and McNally 2007). To provide a realistic spinup of the bias correction predictor coefficients (i.e., mimicking a real-time operational system) for these retrospective satellite assimilation impact tests, an extensive retrospective spinup run was completed to obtain more statistically reliable bias correction bias coefficients for the predictors for all radiance data used. The air mass and scan-angle bias coefficient files used to initialize the bias correction spinup were obtained from the GDAS during July 2012. A preliminary 9-day (8–16 May 2010) retrospective run using multiple applications (W.-S. Wu 2011, personal

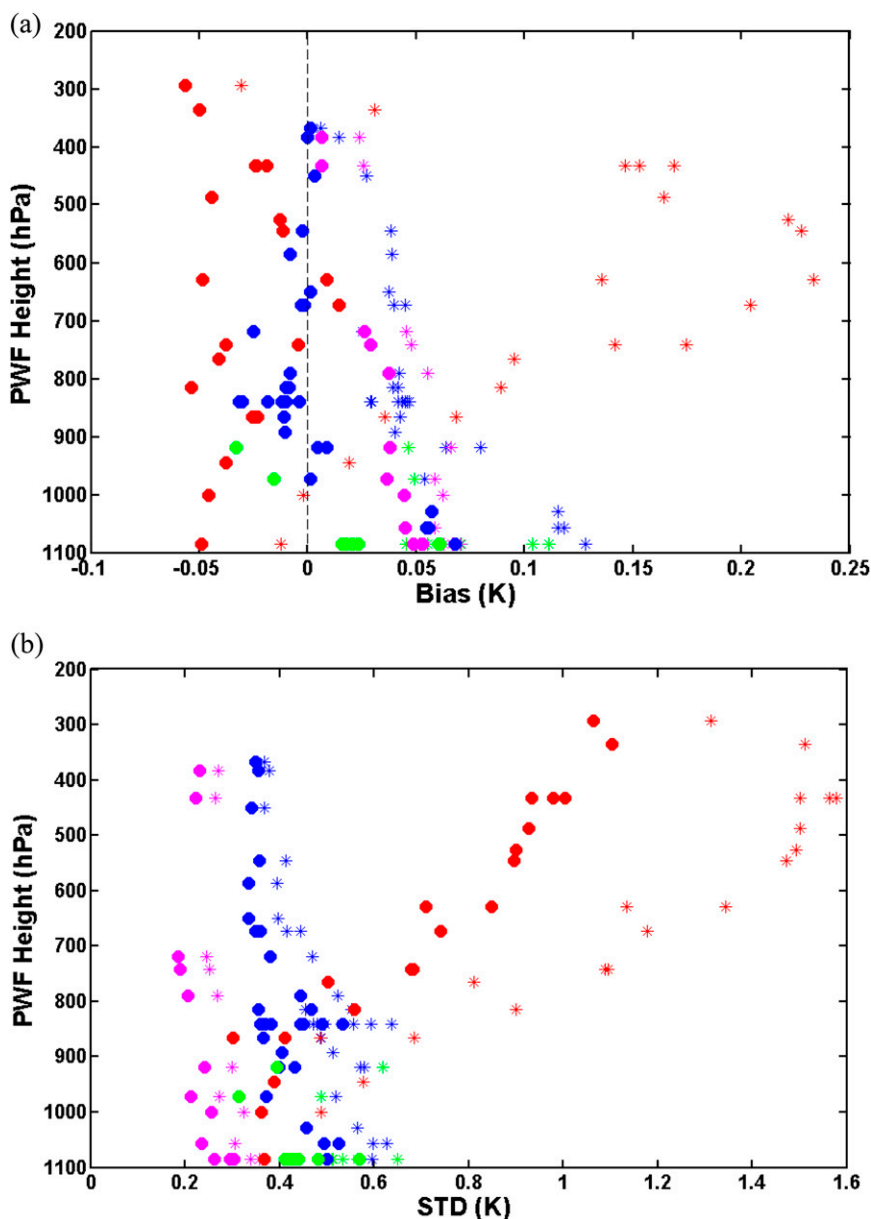


FIG. 7. (a) Mean O-B (K; shown by \*) and O-A (filled circles) and (b) O-B standard deviation errors (\*) and O-A standard deviation errors (filled circles) averaged over the 1-month AIRS experiment. The channels are arranged vertically by PWF height, with blue indicating long-wave carbon dioxide channels, green indicating surface channels, red indicating water vapor channels, and magenta indicating shortwave carbon dioxide channels.

communication) of the GSI per cycle was performed to spin up the bias coefficients. The benefit of this spinup effort was seen in a 9-day AIRS retrospective test completed as part of this study. When the spunup bias coefficients were used, forecast skill improved and more observations were assimilated compared to the case when bias coefficients were not spun up. In this spinup procedure, at each analysis time, updates of both the scan-angle bias coefficients and airmass bias coefficients

are repeated for 30 GSI iterations (i.e., for each iteration, airmass bias coefficients are dynamically updated by running GSI, followed by updating the scan-angle bias coefficients outside of the GSI). The coefficients resulting from this 30-iteration procedure become the starting coefficients for the next analysis time. The updated airmass and scan-angle bias coefficient files after the 9-day spinup are used as the initial bias coefficient files for both the CNTL and EXP runs. It is noted that

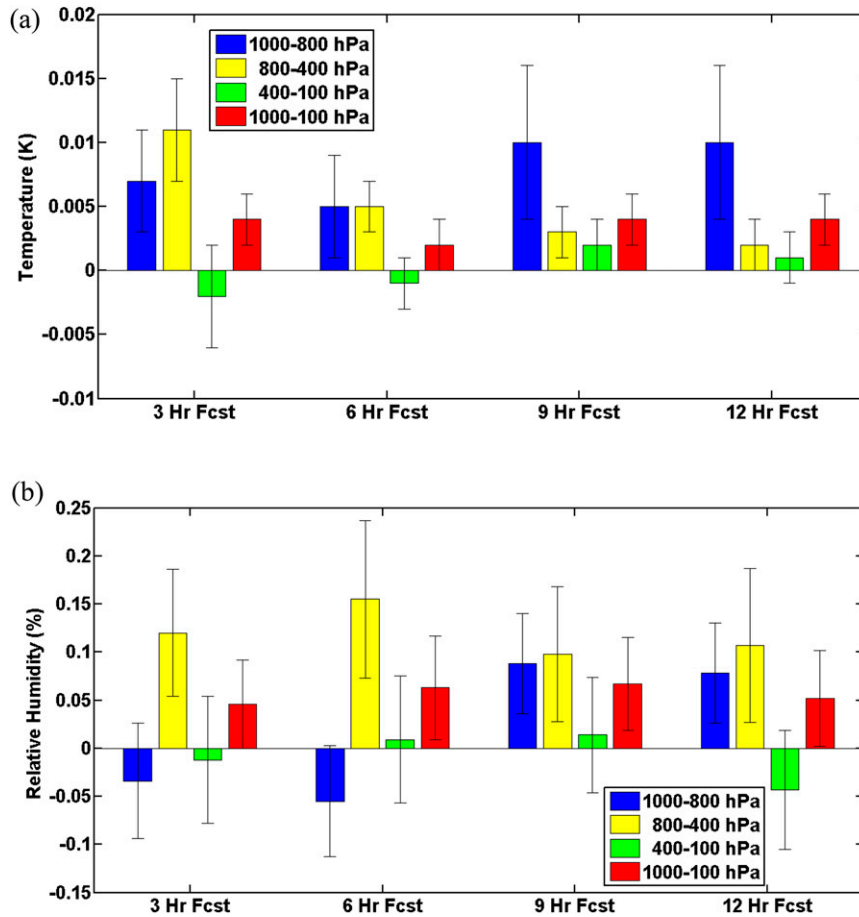


FIG. 8. Difference in RMS errors (vs radiosonde) between the AIRS experiment and the control run for (a) temperature (K) and (b) moisture (%) for different vertical layers (1000–800 hPa, blue; 800–400 hPa, yellow; 400–100 hPa, green; 1000–100 hPa, red) computed against available radiosonde observations over North America over a 1-month period. The error bar indicates the  $\pm 2$  standard error from the mean impact, representing the 95% confidence threshold for significance.

the two-step bias correction procedure used in this paper follows the version used in the older versions of RAP (RAPv1 and RAPv2). RAPv3 (operationally implemented on August 2016) is using the new enhanced variational bias correction scheme developed at NCEP and described by Zhu et al. (2014). The readers are referred to Lin et al. (2017) for more details of the application of the enhanced bias correction scheme in RAPv3.

Bias performance is evaluated by examining histograms of the observation innovations (O-B). We evaluate the effectiveness of the bias correction by examining the mean of the innovation distribution before and after the bias correction. Ideally, the mean should be very close to zero after the bias correction, indicating that the bias correction is working well. For several representative AIRS channels, Fig. 4 shows the

histograms of the brightness temperature (BT) O-B values before (blue) and after (red) application of BC. After BC, the mean values of O-B are closer to zero for these channels compared with the mean O-B values before BC. This demonstrates that the BC procedure is functioning properly. Then, we further to look at examples of the spatial patterns of the bias correction. Figure 5 shows the O-B bias with and without bias correction for AIRS channel 252 (temperature channel) and 1382 (water vapor channel). It can be seen that after bias correction, most large O-B residuals (mainly cold bias) are reduced. Figure 6 shows the mean BT O-B values averaged over a 1-month period before and after the BC for all of the 68 AIRS channels used, arranged according to their PWF height. The mean O-B values for all channels used are also very close to zero after BC, further indicating that the BC is functioning correctly.

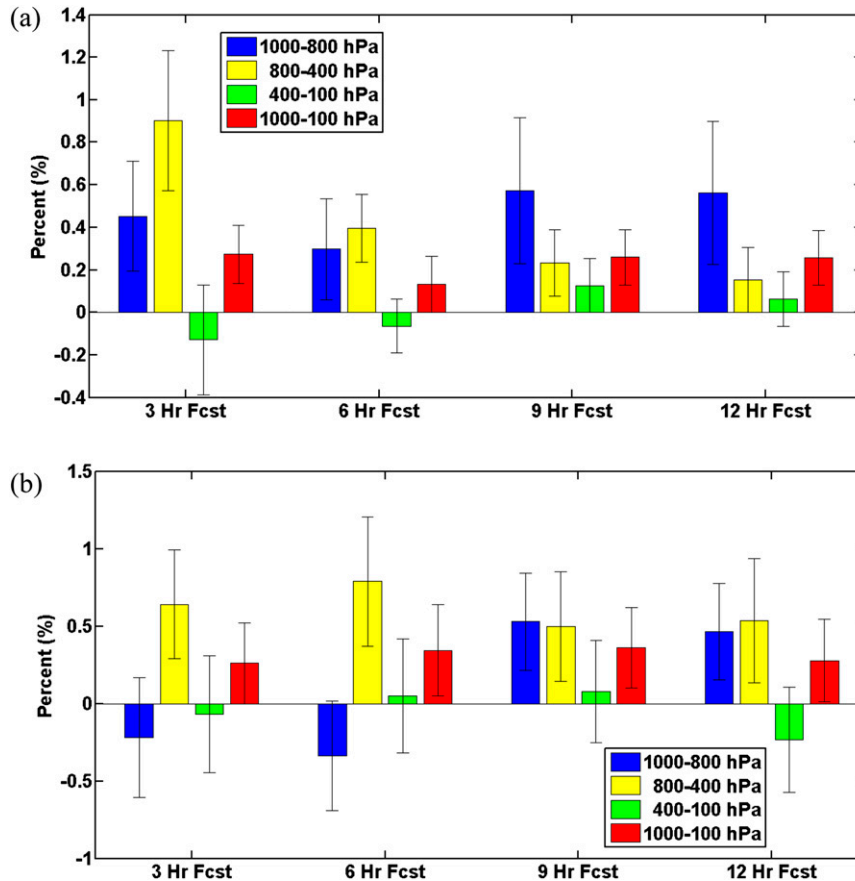


FIG. 9. As in Fig. 8, but for the normalized impact (%).

Longwave carbon dioxide channels (blue) have the largest cold bias ( $-4$  K) before BC for those channels that peaked between 700 and 900 hPa. It is noted that the largest  $-4$ -K bias came from two ozone contamination channels (channels 256 and 257). These two channels have weak ozone-absorbing lines and the WRF-ARW does not have ozone information, which resulted in the large O-B biases. Based on these results, we are going to remove these two channels from our future RAP implementation. The water vapor channels peaking (around 400 hPa) have the largest warm biases, greater than 1 K before application of BC.

## 4. Experiment results

### a. Analysis statistics

Before examining the forecast impact from the assimilation of the bias-corrected AIRS data, we first evaluate analysis statistics by comparing the O-B and analysis errors [observation  $O$  – analysis  $A$  (O-A)] after bias correction. When the average of the analysis errors

(O-A) after BC is close to zero, we can say that the analysis results fit the radiance observations well and the standard deviation of the O-A should certainly be less than the standard deviation of the O-B. Figure 7 shows the mean and standard deviation of O-B (star symbols) and O-A (filled cycles) after BC for all AIRS channels assimilated, arranged according to the height of their PWF. Note that the star symbols in Fig. 7a correspond to the filled circles in Fig. 6 (the range of values in the abscissa is much smaller in Fig. 7a). As can be seen in Fig. 7, the mean biases and standard deviations of the O-A values for different channels are notably smaller than the corresponding values for the O-B values. In Fig. 7a, most O-A bias values (filled circles) are within the range of  $\pm 0.05$  K, while O-B values are as large as 0.25 K for water vapor channels (red stars), indicating these observations were drier than the first guess even after the bias correction. The O-A biases were negative for most of the  $15\text{-}\mu\text{m}$  longwave carbon dioxide channels (blue), indicating that the observations were cooler than the analysis. The O-A biases for most water vapor channels were negative, indicating that the

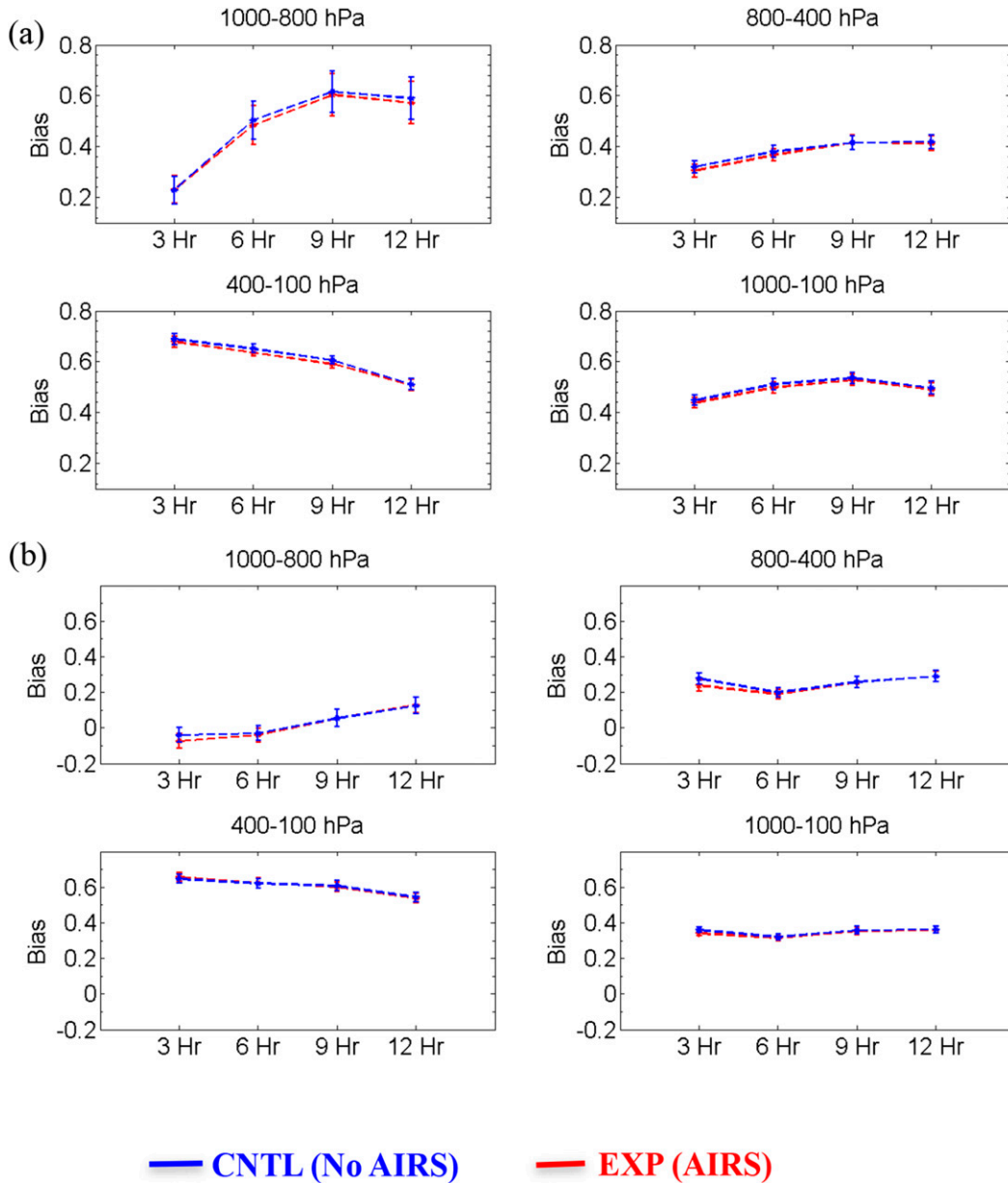


FIG. 10. Temperature bias (K) valid at (a) 0000 and (b) 1200 UTC for radiosonde verification for CNTL (no AIRS; blue) and EXP (AIRS; red) at different forecast hours for different vertical layers with the error bar indicated ( $\pm 1.96$  standard error).

observations were moister than the analyses. Figure 7b shows that after assimilation the O-A standard deviation is significantly reduced relative to the O-B standard deviations, indicating the closer fit to the observations for the analysis compared to the background. The 4.3- $\mu\text{m}$  shortwave carbon dioxide channels (magenta filled) have the smallest O-A standard deviations (around 0.2–0.3 K), followed by the 15- $\mu\text{m}$  shortwave carbon dioxide channels (blue filled) at around 0.4–0.5 K. Most of the surface channels have

standard deviation values around 0.4–0.6 K. The water vapor channels have the largest O-A standard deviations, ranging between 0.3 and 1.1 K, with larger standard deviation for stronger absorption channels. The O-A standard deviation values calculated in this study are similar to those in Lim et al. (2014).

*b. Forecast verification*

We examined the short-term (up to 12 h) forecast impact from the assimilation of the AIRS data by

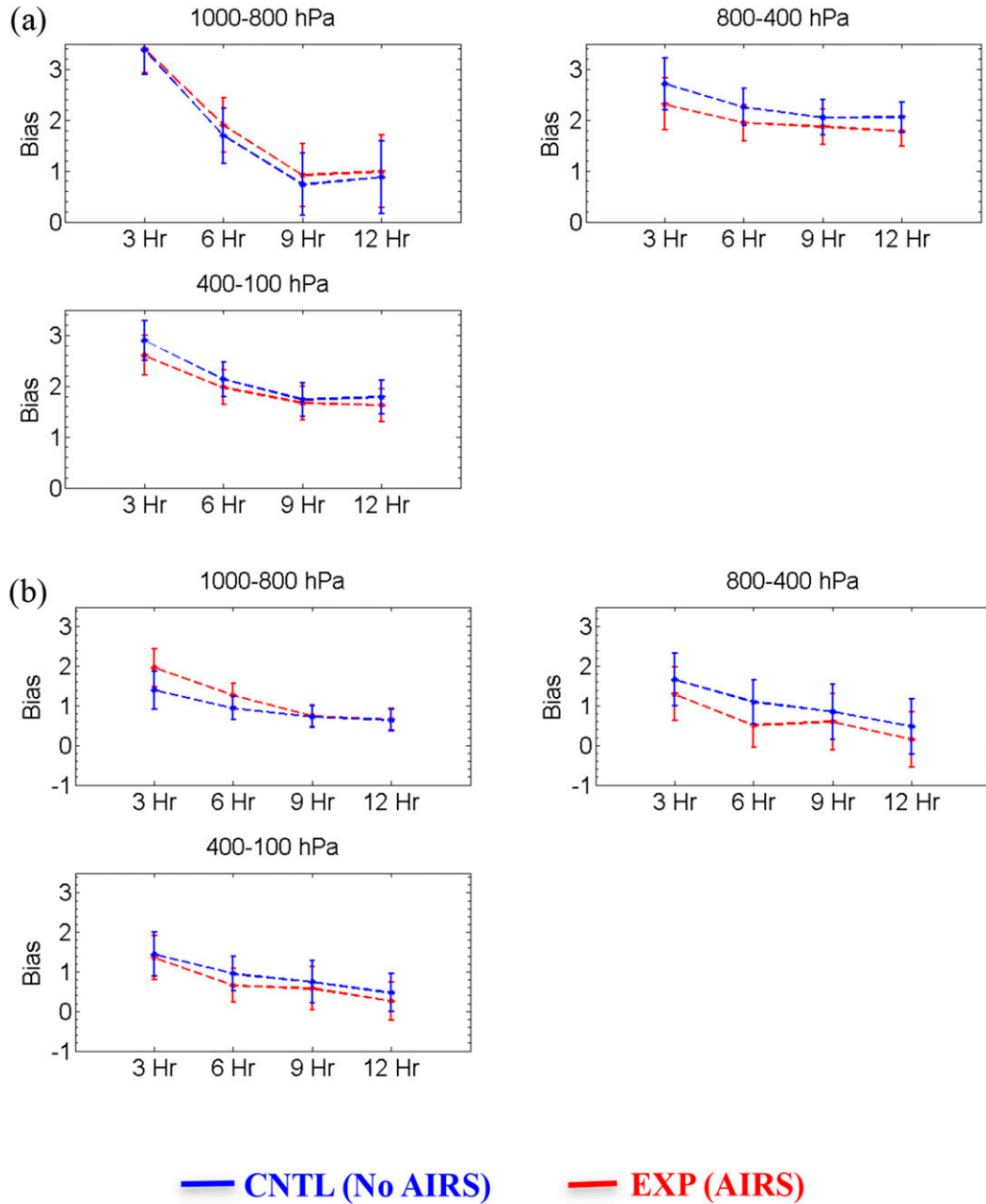


FIG. 11. As in Fig. 10, but for relative humidity (%).

verifying forecasts against radiosonde measurements, METAR surface data, NCEP Stage IV precipitation, and satellite radiance observations. The verification procedures have already been presented in section 2c, and the results presented represent the average scores from a month-long 3-hourly cycled retrospective study with a 12-h forecast every 3 h (245 forecasts).

Figures 8 and 9 show the 3-, 6-, 9-, and 12-h forecast actual and normalized impacts (%) for temperature and

relative humidity RMS errors (verified against radiosonde observations) for different atmospheric layers. Assimilation of clear-sky AIRS radiance data has an overall small positive impact for most layers and forecast hours for temperature and relative humidity. For the normalized temperature impact (Fig. 9a), the biggest positive impact (0.9%) was observed for the 800–400-hPa layer at the 3-h forecast. Overall, small but statistically significant (at the 95% level) positive

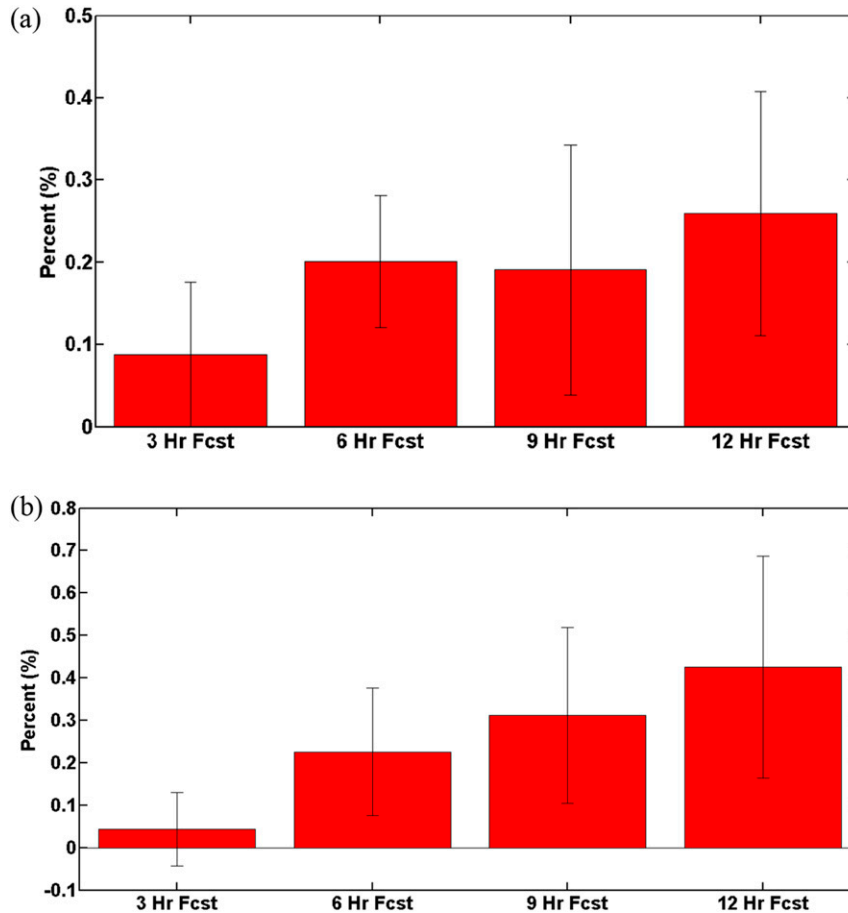


FIG. 12. Normalized impact (%) from EXP (with AIRS) for (a) 2-m temperature and (b) 2-m dewpoint for different forecast hours against near-surface data from METARs over the CONUS domain. The error bar indicates the  $\pm 2$  standard error from the mean impact, representing the 95% confidence threshold for significance.

impacts were seen for temperature for nearly all layers and forecast lengths, with the only exception being short-range forecasts at the upper levels. Slight degradation was noted for temperature at the 3- and 6-h forecasts for the 400–100-hPa layer but these results were not statistically significant. For moisture (Fig. 9b), a consistent (with forecast lead time), statistically significant positive impact was noted for the 800–400-hPa layer. The 1000–800-hPa layer showed a slightly negative forecast impact (but not statistically significant) for the 3- and 6-h forecasts. A possible explanation for this might be bias introduced by the near-surface water vapor channels.

Figures 10a and 10b show the temperature bias verification (also against radiosonde observations) for different atmospheric layers from 3- to 12-h forecasts valid at 0000 and 1200 UTC, respectively. There is a very slight improvement in temperature bias for all layers at

most forecast hours. Figure 11 shows a similar plot to Fig. 10 but for relative humidity bias. Similar to increased low-level relative humidity RMS errors for the AIRS assimilation experiment (Figs. 8b and 9b), the larger relative humidity bias for the 1000–800-hPa layer in the AIRS experiment may be due to bias introduced from the near-surface water vapor channels. For the 800–400-hPa and 1000–400-hPa layer relative humidity, the forecast biases with the assimilation of AIRS data (red) are improved compared with the control run (blue). It is also noted that the temperature and relative humidity biases for forecasts valid at 0000 UTC are larger than those for forecasts valid at 1200 UTC, especially for the 1000–800-hPa layer. This is likely due to the warm temperature bias at 0000 UTC in RAPv2 (see B16).

Figure 12 shows the 3-, 6-, 9-, and 12-h forecast normalized impact (%) for 2-m temperature (Fig. 12a) and 2-m dewpoint (Fig. 12b) against METAR surface

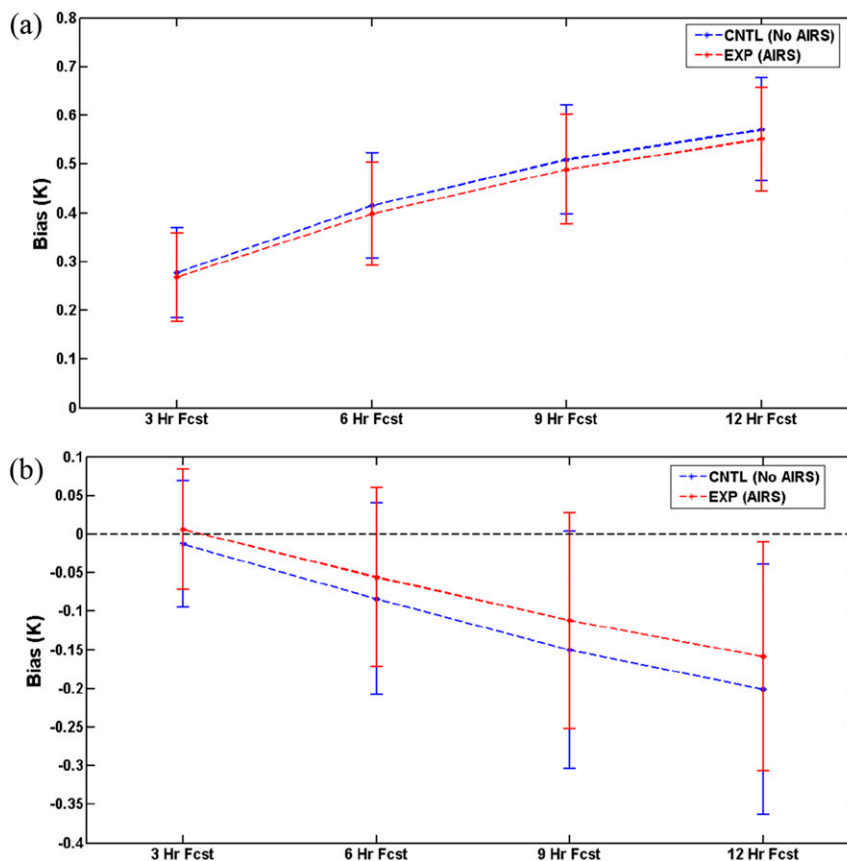


FIG. 13. Bias of (a) 2-m temperature and (b) 2-m dewpoint for METARs surface verification for CNTL (no AIRS; blue) and EXP (AIRS; red) at different forecast hours. The error bar indicates the  $\pm 2$  standard errors from the mean bias (errors), representing the 95% confidence threshold for significance.

observations. AIRS data have a small positive impact on surface temperature and dewpoint verification for all forecast hours with statistically significant (at the 95% level) impacts for 6, 9, and 12 h. The surface temperature and dewpoint biases are also reduced for all forecast hours (Fig. 13).

The CSI, a categorical verification skill measure, is used to evaluate differences in precipitation forecast skill between the different experiments. CSI scores for 24-h accumulated precipitation for the eastern and western United States and biases (forecast area/observation area) are illustrated in Fig. 14. The 24-h accumulated precipitation from the model (on its 13-km grid) is calculated using the 3-h forecasts from eight successive cycles spanning a 1200–1200 UTC period each day. This  $8 \times 3$  h verification procedure was chosen because of the 3-h cycle being used in this experiment; the RAP soil conditions evolve continuously based on the 0–3-h atmospheric forecasts (precipitation, temperature, etc.) as described in B16 (their section 2 and Table 3). From Fig. 14, it is

apparent that the model tends to produce areas of light precipitation that are too widespread, as well as insufficient heavy precipitation. The assimilation of the AIRS radiances yields a slightly positive impact on forecast skill as measured by CSI for the heavier amounts and a negligible impact otherwise.

Last, comparisons are made between model–forecast brightness temperatures generated using CRTM and observed satellite radiance brightness temperatures with no bias correction. Figure 15 shows the mean bias of O-F with no bias correction for different NOAA-18 AMSU-A channels at different forecast hours averaged over the 1-month period (note that the ordinate range varies significantly for the different channels). Mean forecast biases were reduced for all channels except near-surface channels 3, 10, and 15. Simulated brightness temperature using the forecast fields was also compared with observations from AMSU-A on NOAA-19 and similar results were obtained. Figure 16 shows the mean bias of O-F with no bias correction for different

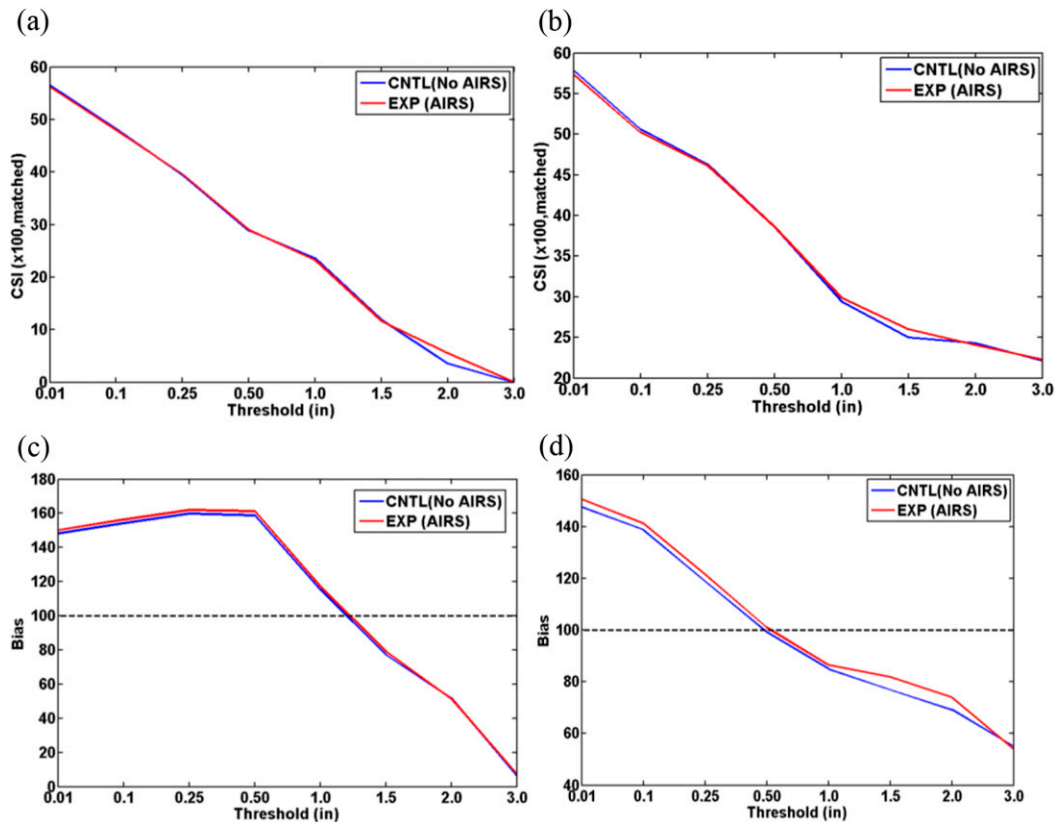


FIG. 14. (a),(b) CSI and (c),(d) bias for 24-h accumulated precipitation ( $8 \times 3$  h totals). Values for the western United States (west of  $100^{\circ}\text{W}$ ) are shown in (a) and (c) and for the eastern United States (east of  $100^{\circ}\text{W}$ ) are shown in (b) and (d). Statistics are computed against NCEP Stage IV precipitation over the 1-month period.

*NOAA-19* MHS channels at different forecast hours averaged over the 1-month period. It is noted that mean forecast biases were reduced for channels 1 and 2, but were large, especially for channel 4 (with PWF height around 454 hPa). The reason may be due to the large bias from the assimilated midlevel (around 600 hPa) AIRS water vapor channels (the red color symbols in Fig. 7).

## 5. Summary

A subset of clear-sky AIRS radiance data was assimilated into a research version of the NOAA Rapid Refresh model system to assess their impact on short-range forecasts during a 1-month retrospective period (1–31 May 2010). The control run included all real-time conventional data and the radiance data from AMSU-A, MHS, and HIRS-4. The AIRS experimental run included all data in the control run plus the AIRS radiance data. To assess the best potential data impact (subject to other limitations in this study), as well as to improve the effectiveness of the radiance bias

correction procedure, all radiance data used in this study were in full coverage (i.e., assumed no data latency and data cutoff issues). Before running the retrospective runs, channel selection and radiance bias correction spinup were performed to improve the effectiveness of the radiance data assimilation in the regional RAP model. Based on an adjoint sensitivity study, a total of 68 AIRS channels were selected from the GDAS channel set for RAP to accommodate its low model top. A 9-day bias correction spinup retrospective run with 30 GSI runs in each cycle was conducted using conventional data and all radiance data to fully spin up the air mass and scan-angle bias coefficients. The updated bias coefficients from the spinup run were used as the starting bias coefficients for both the control and the AIRS experiment runs.

Performance of the bias correction was assessed by looking at observation innovations before and after BC. Results indicated that the mean of the observation innovations for all channels used are close to zero after BC and the histograms of the observation innovations exhibited approximate Gaussian distributions. The

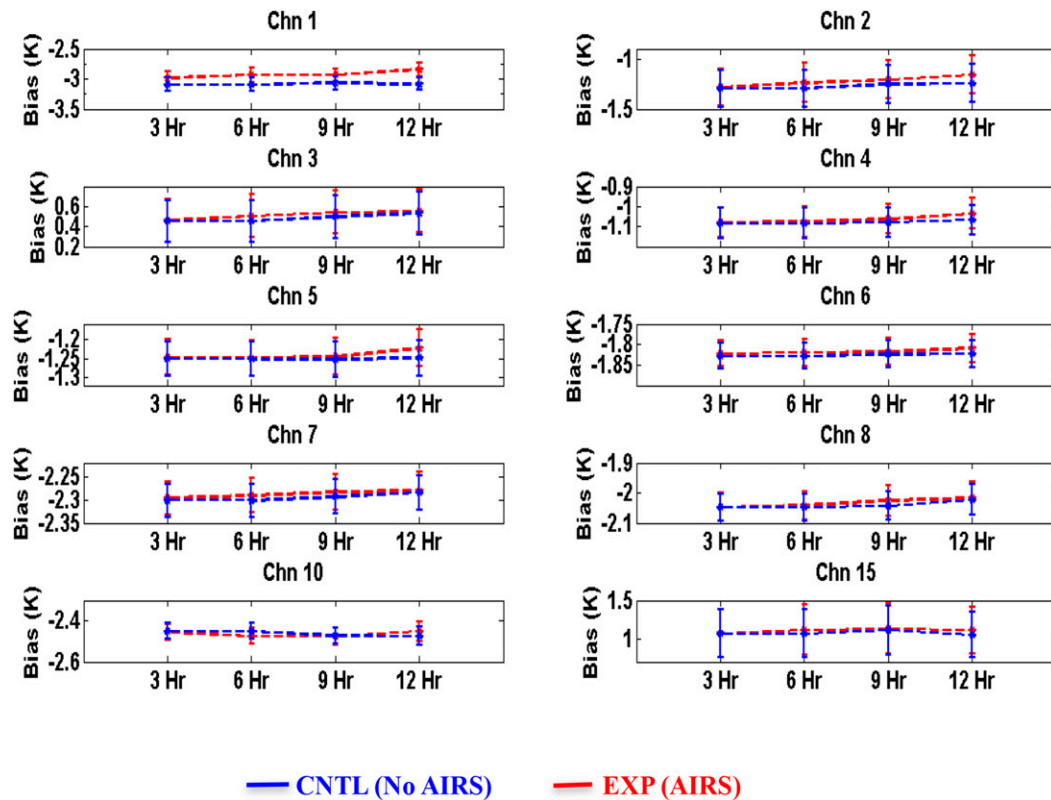


FIG. 15. Bias between observed and simulated BT (AIRS, red; no AIRS, blue) for selected channels on NOAA-18 AMSU-A at different forecast hours with the error bar indicated ( $\pm 1.96$  standard error). Statistics are obtained from the 1-month period (May 2010).

AIRS observations were warmer and drier than the RAP background prior to the BC. The standard deviation of O-A was reduced compared to the standard deviation of the O-B for all channels, indicating the impact of the AIRS observations on the analysis. The AIRS 4.3- $\mu\text{m}$  shortwave carbon dioxide channels had the smallest O-A standard deviations while the water vapor channels had the largest standard deviations, especially for high-peaking channels.

Short-range (3–12 h) forecast verification against radiosonde observations showed a statistically significant positive impact at the 95% confidence threshold from the assimilation of AIRS data. For deep atmospheric layers (1000–100 hPa for temperature and 1000–400 hPa for relative humidity), positive normalized impact (with the largest impact nearly 0.3% and 0.6% respectively) is achieved for temperature and moisture for all forecast hours. METAR surface data verification shows a small positive normalized impact (less than 0.5%) for 2-m temperature and 2-m dewpoint at all forecast hours. Surface temperature and dewpoint biases were reduced for the AIRS experiment compared with the control run. A slightly positive impact was found for higher

threshold precipitation verification against the NCEP Stage IV precipitation data. Comparison of the control run and AIRS assimilation run against AMSU-A data indicated a small bias improvement from the AIRS assimilation for most AMSU-A comparison channels. Exceptions were noted for several surface and upper-level channels when comparing the simulated brightness temperature (from forecast fields) to the observed AMSU-A satellite measurements.

As described in section 1, the results from this study represent upper limits (subject to other limitations in this study) on the forecast improvements to be expected when using AIRS data within RAP because full-coverage data were used. The 1-month length of the retrospective study, the use of a full suite of other observations, and the completion of the tests using a close to operational version of RAP all lend credibility to the robustness of the results reported.

This paper also includes a description of the application of the original NCEP cycled variational bias correction scheme (Derber and Wu 1998; Dee 2005) to the RAP hourly updated model. Application of this bias correction to RAP is very similar to the application of the enhanced

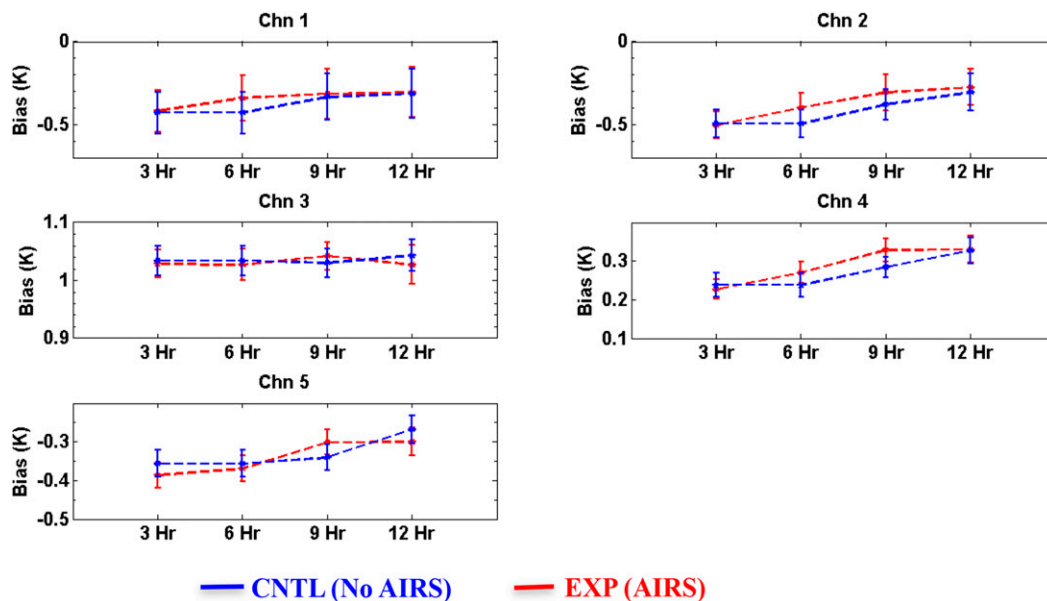


FIG. 16. As in Fig. 15, but from the NOAA-19 MHS.

NCEP bias correction (Zhu et al. 2014) that was implemented with RAPv3 in August 2016, and this work provided a basis for the RAP-specific bias correction procedures applied to other satellite radiance data now used in the NCEP operational RAPv3. The paper also describes initial results for channel selection and assimilation of hyperspectral radiance data into RAP, and this work provided a basis for RAP-specific channel selection procedures applied to other satellite radiance data used in the NCEP operational RAPv3. The AIRS radiance assimilation described here sets the stage for an overall radiance assimilation impact study within RAPv3 (Lin et al. 2017).

This study has demonstrated that assimilation of AIRS data into the RAP model system yields a small but statistically significant positive impact on short-range (3–12 h) forecasts. Based on these results, assimilation of AIRS radiance data into the NOAA-operational RAP can potentially further improve operational RAP forecasts if data latency and data cutoff issues for real-time implementation can be addressed. As a result of the data latency and short cutoff time, the real-time hourly AIRS data coverage for RAP was quite limited, and AIRS data were not included in RAPv3. But recent modifications to the experimental RAP configuration allow for a delay in the starting time for many of the partial cycles (0300–0700 and 1500–2000 UTC), thereby increasing the amount of AIRS data available in real time. Based on these positive results from this paper and this configuration change, AIRS data assimilation is planned for RAPv4 along with other new radiance datasets [e.g., IASI, Cross-track Infrared Sounder (CrIS), and Advanced Technology Microwave Sounder (ATMS)].

*Acknowledgments.* This work was supported by NOAA Award NA090AR4320074. The views, opinions, and findings contained in this report are those of the authors and should not be construed as an official National Oceanic and Atmospheric Administration or U.S. government position, policy, or decision. The authors thank Dr. Daniel Birkenheuer and John Osborn of NOAA/ESRL/GSD, and three anonymous reviewers, for their very helpful reviews of this manuscript.

## REFERENCES

- Auigné, T., and A. P. McNally, 2007: Interaction between bias correction and quality control. *Quart. J. Roy. Meteor. Soc.*, **133**, 643–653, doi:10.1002/qj.57.
- , —, and D. P. Dee, 2007: Adaptive bias correction for satellite data in a numerical weather prediction system. *Quart. J. Roy. Meteor. Soc.*, **133**, 631–642, doi:10.1002/qj.56.
- Aumann, H. H., and Coauthors, 2003: AIRS/AMSU/HSB on the Aqua mission: Design, science objectives, data products, and processing systems. *IEEE Trans. Geosci. Remote Sens.*, **41**, 253–264, doi:10.1109/TGRS.2002.808356.
- Benjamin, S. G., and Coauthors, 2004a: An hourly assimilation/forecast cycle: The RUC. *Mon. Wea. Rev.*, **132**, 495–518, doi:10.1175/1520-0493(2004)132<0495:AHACTR>2.0.CO;2.
- , B. E. Schwartz, E. J. Szoke, and S. E. Koch, 2004b: The value of wind profiler data in U.S. weather forecasting. *Bull. Amer. Meteor. Soc.*, **85**, 1871–1886, doi:10.1175/BAMS-85-12-1871.
- , B. D. Jamison, W. R. Moninger, S. R. Sahn, B. Schwartz, and T. W. Schlatter, 2010: Relative short-range forecast impact from aircraft, profiler, radiosonde, VAD, GPS-PW, METAR, and mesonet observations via the RUC hourly assimilation cycle. *Mon. Wea. Rev.*, **138**, 1319–1343, doi:10.1175/2009MWR3097.1.
- , and Coauthors, 2016: A North American hourly assimilation and model forecast cycle: The Rapid Refresh. *Mon. Wea. Rev.*, **144**, 1669–1694, doi:10.1175/MWR-D-15-0242.1.

- Cameron, J., A. Collard, and S. English, 2005: Operational use of AIRS observations at the Met Office. *14th Int. TOVS Study Conf.*, Beijing, China, Int. ATOVS Working Group, [https://cimss.ssec.wisc.edu/itwg/itsc/itsc14/proceedings/B25\\_Cameron.pdf](https://cimss.ssec.wisc.edu/itwg/itsc/itsc14/proceedings/B25_Cameron.pdf).
- Chen, Y., F. Weng, Y. Han, and Q. Liu, 2008: Validation of the community radiative transfer model by using CloudSat data. *J. Geophys. Res.*, **113**, D00A03, doi:10.1029/2007JD009561.
- Dee, D. P., 2005: Bias and data assimilation. *Quart. J. Roy. Meteor. Soc.*, **131**, 3323–3343, doi:10.1256/qj.05.137.
- Derber, J. C., and W.-S. Wu, 1998: The use of TOVS cloud-cleared radiances in the NCEP SSI analysis system. *Mon. Wea. Rev.*, **126**, 2287–2299, doi:10.1175/1520-0493(1998)126<2287:TUOTCC>2.0.CO;2.
- Goldberg, M. D., Y. Qu, L. McMillin, W. Wolf, L. Zhou, and M. Divakarla, 2003: AIRS near-real-time products and algorithms in support of operational numerical weather prediction. *IEEE Trans. Geosci. Remote Sens.*, **41**, 379–389, doi:10.1109/TGRS.2002.808307.
- Han, Y., P. van Delst, Q. Liu, F. Weng, B. Yan, R. Treadon, and J. Derber, 2006: JCSDA Community Radiative Transfer Model (CRTM) version 1. NOAA Tech. Rep. NESDIS 122, 31 pp., [http://www.emc.ncep.noaa.gov/research/JointOSSE/Manuals/CRTM\\_v1\\_NOAAtechReport.pdf](http://www.emc.ncep.noaa.gov/research/JointOSSE/Manuals/CRTM_v1_NOAAtechReport.pdf).
- Joo, S., J. Eyre, and R. Marriott, 2013: The impact of MetOp and other satellite data within the Met Office global NWP system using an adjoint-based sensitivity method. *Mon. Wea. Rev.*, **141**, 3331–3342, doi:10.1175/MWR-D-12-00232.1.
- Kleist, D. T., D. F. Parrish, J. C. Derber, R. Treadon, W.-S. Wu, and S. Lord, 2009: Introduction of the GSI into the NCEP Global Data Assimilation System. *Wea. Forecasting*, **24**, 1691–1705, doi:10.1175/2009WAF2222201.1.
- Le Marshall, J., and Coauthors, 2006: Improving global analysis and forecasting with AIRS. *Bull. Amer. Meteor. Soc.*, **87**, 891–894, doi:10.1175/BAMS-87-7-891.
- Lim, A. H. N., J. A. Jung, H.-L. A. Huang, S. A. Ackerman, and J. A. Otkin, 2014: Assimilation of clear sky Atmospheric Infrared Sounder radiances in short-term regional forecasts using community models. *J. Appl. Remote Sens.*, **8**, 083655, doi:10.1117/1.JRS.8.083655.
- Lin, H., S. S. Weygandt, S. G. Benjamin, and M. Hu, 2017: Satellite radiance data assimilation within the hourly updated Rapid Refresh. *Wea. Forecasting*, **32**, 1273–1287, <https://doi.org/10.1175/WAF-D-16-0215.1>.
- Lin, Y., and K. E. Mitchell, 2005: The NCEP Stage II/IV hourly precipitation analyses: Development and applications. *19th Conf. on Hydrology*, San Diego, CA, Amer. Meteor. Soc., 1.2, <https://ams.confex.com/ams/pdfpapers/83847.pdf>.
- McCarty, W., G. Jedlovec, and T. L. Miller, 2009: Impact of the assimilation of Atmospheric Infrared Sounder radiance measurements on short-term weather forecasts. *J. Geophys. Res.*, **114**, D18122, doi:10.1029/2008JD011626.
- McNally, A. P., P. D. Watts, J. A. Smith, R. Engelen, G. A. Kelly, J. N. Thépaut, and M. Matricardi, 2006: The assimilation of AIRS radiance data at ECMWF. *Quart. J. Roy. Meteor. Soc.*, **132**, 935–957, doi:10.1256/qj.04.171.
- Moninger, W. R., S. G. Benjamin, B. D. Jamison, T. W. Schlatter, T. L. Smith, and E. J. Szoke, 2010: Evaluation of regional aircraft observations using TAMDAR. *Wea. Forecasting*, **25**, 627–645, doi:10.1175/2009WAF2222321.1.
- Ota, Y., J. C. Derber, E. Kalnay, and T. Miyoshi, 2013: Ensemble-based observation impact estimates using the NCEP GFS. *Tellus*, **65A**, 20038, doi:10.3402/tellusa.v65i0.20038.
- Ruston, B., C. Blankenship, W. Campbell, R. Langland, and N. Baker, 2006: Assimilation of AIRS data at NRL. *15th Int. TOVS Study Conf.*, Maratea, Italy, Int. ATOVS Working Group, 156–161, [http://cimss.ssec.wisc.edu/itwg/itsc/itsc15/proceedings/7\\_2\\_Ruston.pdf](http://cimss.ssec.wisc.edu/itwg/itsc/itsc15/proceedings/7_2_Ruston.pdf).
- Schaefer, J. T., 1990: The critical success index as an indicator of warning skill. *Wea. Forecasting*, **5**, 570–575, doi:10.1175/1520-0434(1990)005<0570:TCSIAA>2.0.CO;2.
- Singh, R., C. M. Kishtawal, S. P. Ojha, and P. K. Pal, 2012: Impact of assimilation of Atmospheric InfraRed Sounder (AIRS) radiances and retrievals in the WRF 3D-Var assimilation system. *J. Geophys. Res.*, **117**, D11107, doi:10.1029/2011JD017367.
- Skamarock, W. C., and Coauthors, 2008: A description of the Advanced Research WRF version 3. NCAR Tech. Note NCAR/TN-475+STR, 113 pp., <http://dx.doi.org/10.5065/D68S4MVH>.
- Susskind, J., C. D. Barnet, and J. Blaisdell, 2003: Retrieval of atmospheric and surface parameters from AIRS/AMSU/HSB data in the presence of clouds. *IEEE Trans. Geosci. Remote Sens.*, **41**, 390–409, doi:10.1109/TGRS.2002.808236.
- Wang, P., and Coauthors, 2015: Assimilation of thermodynamic information from advanced infrared sounders under partially cloudy skies for regional NWP. *J. Geophys. Res. Atmos.*, **120**, 5469–5484, doi:10.1002/2014JD022976.
- Weng, F. Z., 2007: Advances in radiative transfer modeling in support of satellite data assimilation. *J. Atmos. Sci.*, **64**, 3799–3807, doi:10.1175/2007JAS2112.1.
- Wu, W.-S., R. J. Purser, and D. F. Parrish, 2002: Three-dimensional variational analysis with spatially inhomogeneous covariances. *Mon. Wea. Rev.*, **130**, 2905–2916, doi:10.1175/1520-0493(2002)130<2905:TDDVAWS>2.0.CO;2.
- Zhu, Y., J. Derber, A. Collard, D. Dee, R. Treadon, G. Gayno, and J. A. Jung, 2014: Enhanced radiance bias correction in the National Centers for Environmental Prediction's Gridpoint Statistical Interpolation data assimilation system. *Quart. J. Roy. Meteor. Soc.*, **140**, 1479–1492, doi:10.1002/qj.2233.